High energy femtosecond OPA pumped by 1030 nm Nd:KGW laser.

V. Kozich[1], A. Moguilevski, and K. Heyne

Institut für Experimentalphysik, Freie Universität Berlin, Arnimallee 14, D-14195 Berlin, Germany

Abstract

We present a traveling-wave-type optical parametric amplifier (OPA) pumped at 1.03 µm by a Yb:KGW laser, that produces tunable high-energy pulses of 6.5 to 4 µJ in the mid-infrared (mid-IR) from 3.6 to 7 µm. Pumping with negatively chirped pulses generates nearly transform-limited (TL) mid-IR pulses of 300-330 fs length. Pumping with TL pulses of 200 fs decreases the output energy by a factor of 1.5, but also decreases the mid-IR pulse-length to 160 fs after additional compression. The new and simple OPA set-up is ideal for femtosecond infrared experiments in the fingerprint region.

Transient vibrational spectroscopy requires tunable short pulses in the range of 1000-3000 cm^{-1}. High energies (on the µJ level) and controllable pulse-lengths and spectral-widths are desirable for selective high vibrational excitation (ladder climbing) as well as for many application requiring sufficient population changes. A widespread approach to generate short tunable pulses at 1-10 µm is based on traveling-wave-type optical parametrical generator (OPG) or amplifier (OPA) pumped with commercial femtosecond Ti:Sapphire laser with a subsequent difference frequency generation (DFG) between signal and idler waves [1-5]. OPA set-ups with longer pump wavelengths, e.g. at 1.03 µm delivered by Yb-doped potassium gadolinium tungstate (Yb:KGW) laser, enable generation of short tunable pulses at 1.2 – 9 µm without using DFG processes. Such an approach for generating short pulses in the mid-IR with about 1µJ pulse energy was realized in [6] by using 1.25 µm pump pulses delivered by a Cr:forsterite regenerative amplifier. In this paper we demonstrate a high-energy OPA based on a silver thiogallate ($AgGaS_2$ or AGS) crystal pumped with a Yb:KGW femtosecond laser.

[1]Corresponding author. Tel: +49-30-83855127
E-Mail address: kozich@zedat.fu-berlin.de

1.Experimental set-up

The scheme of the OPA is depicted in Fig.1. The set-up is based on a commercial Yb:KGW laser (Pharos, Light Conversion Ltd.) providing about 1000 µJ pulse energy at a pulse duration of 200 fs and at repetition rate of 2 kHz. We used 400 µJ pulses to pump the OPA. A white-light continuum generated from 3 µJ pulses in a 2-mm sapphire window seeds a 5-mm-thick, type II β-barium borate (BBO) in the first amplification stage of the OPA. This amplification stage is pumped by 40-50 µJ pulses of a second harmonic (SH) at 515 nm, generated from the fundamental in a 1-mm BBO-crystal. We use BBO-crystal to gain the seed because it has weaker self-phase modulation and group-velocity dispersion effects, in comparison with AGS. The amplified seed in the spectral range 1.15 - 1.46 µm is further amplified by a second amplification stage in a 2-mm-thick, type II AGS crystal. This crystal is pumped by about 27 µJ pulses at 1.03 µm tightly focused by a f=50 cm lens. In this step we generate additionally an idler wave in the spectral range of 3.5 - 9 µm. The seed pulses are reflected by a concave mirror with radius R=20 cm back to the crystal and the second pass in AGS is pumped by 260 µJ pulses at 1.03 µm. Adjusting the beam waist with a 1:2 telescope, we obtain nearly collimated pump beams with a diameter of about 1 mm and a peak intensity of I_0=90-170 GW/cm^2 depending on the laser regime (stretched or transform-limited pump pulses).

The restriction on the conversion efficiency in an OPA with very different signal and idler wavelengths as, for example, in the case of 1.03 µm $\rightarrow$ 1.33 µm + 4.6 µm, is mostly due to the group velocity mismatch (GVM) and group velocity dispersion (GVD) [7-9]. The GVM in the above example in AGS, type II is about -100 fs/mm between pump and signal and -450 fs/mm between pump and idler pulses [10]. It is well known that, to approach transform-limited pulse-width in an OPG, signal and idler pulses must walk in opposite directions with respect to the pump [11]. It was shown that if signal and idler pulse walk in opposite directions, the time-bandwidth product remains close to the transform-limited value, but it increases if they begin to walk in the same direction. In the latter case the output efficiency drops, but the spectral width increases [12].

We have used two approaches depending on the OPA's applications: negative chirped and transform-limited pump pulses.

2. Chirped pump pulse

The first approach is aimed to achieve maximum output energy.

We have optimized the output power of OPA by varying the compressor settings in the commercial Yb:KGW femtosecond laser Pharos. The OPA is sensitive to such variations and one needs to optimize simultaneously the delays of the pump pulses at all stages of the OPA.

The pulse-width at 1.03 μm was measured with a commercial autocorrelator APE (Angewandte Physik & Elektronik GmbH). To check the width of IR pulses we used a home-built autocorrelator. Our autocorrelator is based on a non-collinear SH generation in 1-mm thick GaSe or AGS crystals. The SH-spectrum is detected by an infrared HORIBA Jobin Yvon spectrometer and a nitrogen cooled HgCdTe array (Infrared System Development Corp.). The measured integrated signal (spectral area) as a function of delay between the two non-collinear infrared beams presents the autocorrelation function.

In Fig.2, the measured autocorrelation functions (ACF) of initial close to transform-limited pulse of Yb:KGW laser (a) and chirped pump pulse (b) are shown. The chirp has been optimized for maximum OPA energy-output at 4.6 μm. The gain in output energy by using chirped pump pulses reaches a factor of 1.5 – 2 for pump-pulse-lengths of about 400-415 fs. We have determined that the optimized pump-pulses have negative chirp by measuring ACFs after passing through two ZnSe wedges having positive GVD=700 fs^2/mm at 1.03 μm. As a result the effective dispersion of the chirped pump of about -26000 fs^2 is estimated assuming that a linear chirp was imposed on the pump pulse.

The ACF of the generated IR pulses at 4.6 μm is shown in the Fig.2(c). The observed oscillations are due to contribution by the interference in the nonlinear SH-crystal. The spectral width (FWHM) of the idler pulse in the range 3.5 - 8 μm varies from $\Delta\nu$ =45 cm^{-1} to 55 cm^{-1}. It depends on non-collinear phase-matching conditions, as well as on group velocity matching. The detailed study at 4.6 μm shows that the time-bandwidth product differs less than 10 % from the transform-limited value assuming Gaussian pulse shape, as, for example, for the measured τ = 330 fs (the ACF is shown in Fig. 2(c)) and $\Delta\nu$ = 46 cm^{-1}. We should stress the result that negatively chirped pulses with rather high effective dispersion enable generation high-energy practically transform-limited IR pulses without additional compression. The negative chirp improves group velocity matching between pump and signal seed pulses, both of which have positive GVD of the magnitude of hundreds fs^2/mm [9], and also works like a precompensation of overall GVD in the OPA system.

In Fig. 3, the tuning range of OPA with chirped pump pulses is displayed. We obtained output energies ≥ 1 μJ for mid-IR idler pulses in the spectral range from 3.5 μm to 8.3 μm, output energies ≥ 4 μJ in the spectral range from 3.6 μm to 7 μm, and maximum output energies of about 6.5 μJ at 4.5-5 μm. Despite the flow of dry air through our OPA-box the drop of the output energy in the range of water and CO_2 absorption, especially in the range of 3 µm can be seen. Comparing the output energies and tuning range with substantially more complex systems based on commercial Ti:Sapphire lasers and OPAs,[5] we achieved similar or even higher output energies.

We have also realized a reduced scheme of OPA with only one amplification pass through the AGS crystal. In this OPA scheme the amplification stage with Delay2 is missing (cp. Fig.1). Such a reduced OPA has the advantage of simple alignment and tuning. The output energy of the reduced OPA, is about 2.4 times lower with 1.6 times lower pump energy. Thus, it exhibits a reduction in efficiency of about 1.5.

3. Transform-limited pump pulse

To generate shorter IR pulses of broader spectral width, we pumped the OPA with the shortest pulse possible in our set-up. As seen in Fig. 2(a), the original pulse-width of the commercial Pharos laser is about 200 fs.

To analyze this regime, we have measured the changes in the parameters of the pump pulse focused to 170 GW/cm^2 after passing through a 2-mm AGS crystal in the last stage of the OPA. The pump pulse was broadened from 200 to 325 fs. The estimated GVD of 630 fs^2/mm is not big enough to explain this broadening. We propose self-phase-modulation as the origin for the additional pulse-broadening. One should note that spectral changes in this case are not so pronounced as changes in ACF-width.

Using TL pump pulses we achieved 4.3 µJ IR pulse energies, about 1.5 times lower than using chirped pump pulses. However, with TL pump pulses a spectral width of 110 cm^{-1} at 4.6 µm was observed, which represents a twofold increase of bandwidth compared to chirped pump pulses. As the IR output pulses are not transform-limited, we used a passive pulse-shaper consisting of two sapphire wedges movable relative to each other to compress the IR pulses [13]. In Fig. 4, we presented ACF of generated IR-pulses at 4.6 µm (a), of compressed pulses with additional 5 mm optical path in sapphire wedges (b), and the best ACF (c) obtained after 10 mm optical path in sapphire wedges.

Using the passive pulse-shaper the initial infrared pulse-width of 314 fs was compressed to a minimum value of 160 fs. We have fitted the change of pulse-parameters upon compression. The compression of the pulse is well described by a complex Gaussian field-envelope $\boldsymbol{E} \propto \boldsymbol{exp}[-(\boldsymbol{t^2}/\boldsymbol{\tau^2} + \boldsymbol{\alpha t^2})/\boldsymbol{2}]$ using a positive linear chirp of $\alpha = -0.000047$ fs^{-2} and a calculated GVD of 1500 fs^2/mm in sapphire. Here, τ is the pulse-width and α is a measure of linear chirp. The initial effective dispersion in this case is about 13500 fs^2.

We should note that the infrared output pulse has positive chirp, despite negative GVD of -80 fs^2/mm in AGS at 4.6 µm [9]. The reason is that the seed pulses at 1.33 µm, as well as the pump pulses have a few times higher positive GVD finally resulting in a positive chirp in the idler wave. We managed to compensate this chirp by a home-built passive pulse-shaper with sapphire wedges showing negative GVD. Thus, we received transform-limited IR pulses of 160 fs pulse length and about 3.2 µJ at 4.6 µm.

3. Conclusions.

We have demonstrated an OPA pumped with 400 µJ pulse energy capable of generating high energy femtosecond pulses in the range from 3.5 to 9 µm without difference frequency generation. We achieved maximal output energies higher than 6 µJ around 5 µm. The pump pulses at 1.03 µm were either negatively chirped or transform- limited.

Negative chirp of the pump pulses increases the output energy by a factor of 1.5 - 2 and enables to generate nearly transform-limited pulses with 280-330 fs pulse length (FWHM).

Pumping with transform-limited pulses generates positively chirped IR pulses of 110 cm^{-1} spectral width, which were compressed to 160 fs using a home-built tunable passive pulse-shaper with a material of negative GVD. For both pump pulses regimes the power of the infrared output pulses were nearly identical upon using the passive pulse-shaper.

Here, we present a new and simple IR OPA set-up without difference frequency generation optimally suited for femtosecond infrared experiments in the fingerprint region.

Acknowledgements

We appreciate the help of T. von Haimberger programming the software of the home-built IR autocorrelator and M. Hartmann for providing the passive pulse-shaper.

References

[1] G. Cerullo and S. De Silvestri, Rev. Sci. Instrum. 74 (2003) 1-18.

[2] T. Kobayashi, J. Liu, and K. Okamura, J. Phys. B: Mol. Opt. Phys. 45 (2012) 074005.

[3] V. Petrov, F. Rotermund, F. Noack, J. Opt. A: Pure Appl. Opt. 3 (2001) R1- R19.

[4] R. A. Kaindl, M. Wurm, K. Reimann, P. Hamm, A. M. Weiner, and M. Woerner, J. Opt. Soc. Am. B 17 (2000) 2086-2094.

[5] F. Rotermund, V. Petrov, F. Noack, Opt. Commun. 185 (2000) 177-183.

[6] F. Rotermund, V. Petrov, Opt. Lett. 25 (2000) 746-748.

[7] A. V. Smith, Opt. Lett. 26 (2001) 719-721.

[8] P. Yuan, L. Qian, H. Luo, H. Zhu, and S. Wen, IEEE J. Sel. Topics Quantum Electron. 12 (2006) 181-186.

[9] J.-C. M. Diels, J. J. Fountaine, I. C. McMichael, and F. Simoni, Appl. Optics 24 (1985) 1270-1282.

[10] SNLO nonlinear optics software at http://www.sandia.gov.

[11] X. Xie, A. M. Schober, C. Langrock, R. V. Roussev, J. R. Kurz, and M. M. Fejer, J. Opt. Soc. Am. B 21 (2004) 1397-1402.

[12] M. Marangoni, R. Osellame, R. Ramponi, G. Cerullo, A. Steinmann, and U. Morgner, Opt. Lett. 32 (2007) 1489-1491.

[13] K. Heyne, M. Hartmann, K. Molkenthin, (2009): WO2009135870: Pulse shaper and laser with pulse shaper. 12.11.2009

Figure captions.

Fig. 1. Scheme of the 3-stages IR-OPA with BBO and AGS crystals. The pump delay at 515 nm in the 1-st stage is adjusted with Delay1, and at 1030 nm in the 2-d and 3-d stages with Delay2 and Delay3.

Fig. 2. Measured autocorrelation functions of Yb:KGW laser (a), chirped pump pulse for the OPA (b), and generated mid-IR pulses at 4.6 μm (c).

Fig. 3. Experimentally obtained mid-IR pulse energies for pumping the OPA by negatively chirped pulses.

Fig. 4. Measured autocorrelation functions of pulses at 4.6 μm for pumping the OPA by transform-limited pulses (a), of compressed pulses after 5 mm (b), and 10 mm (c) path in sapphire wedges.

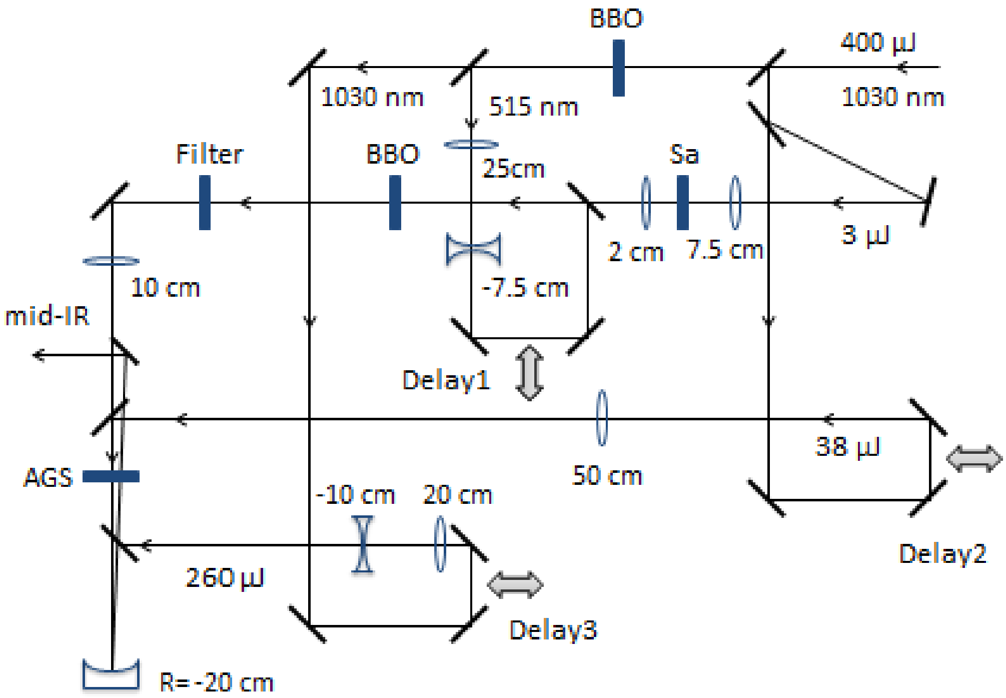
BBO
400 µJ
1030 nm
1030 nm
515 nm
Filter
BBO
25cm
Sa
2 cm
7.5 cm
3 µJ
10 cm
-7.5 cm
mid-IR
Delay1
50 cm
38 µJ
AGS
-10 cm
20 cm
260 µJ
Delay2
Delay3
R=-20 cm

Fig.1

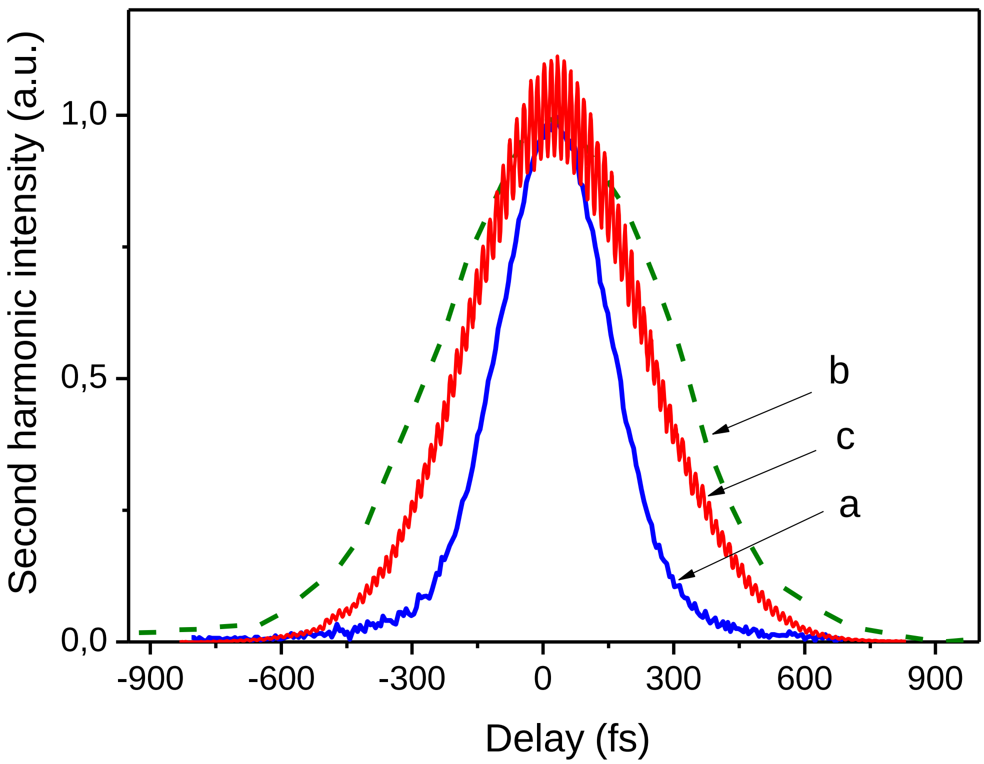
Second harmonic intensity (a.u.)
1,0
0,5
0,0
-900
-600
-300
0
300
600
900
Delay (fs)
b
c
a

Fig.2

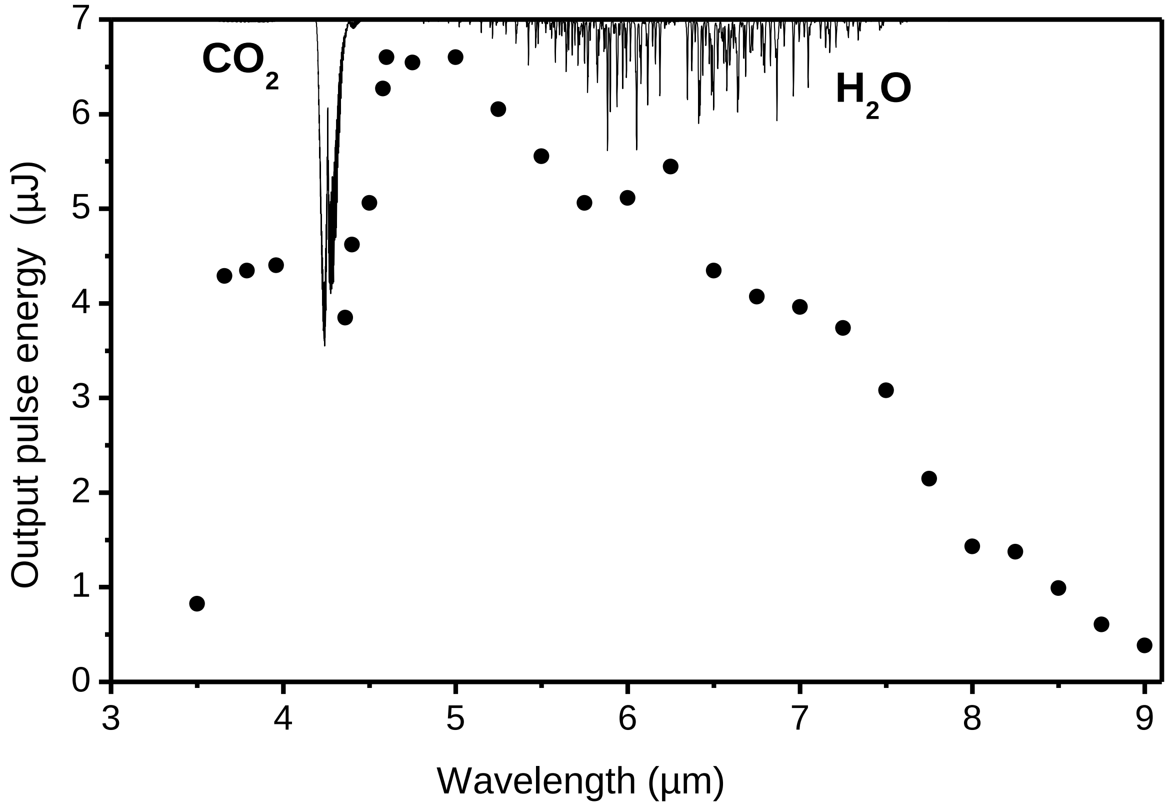

Output pulse energy (μJ)
Wavelength (μm)
CO_2
H_2O
0
1
2
3
4
5
6
7
3
4
5
6
7
8
9

Fig.3

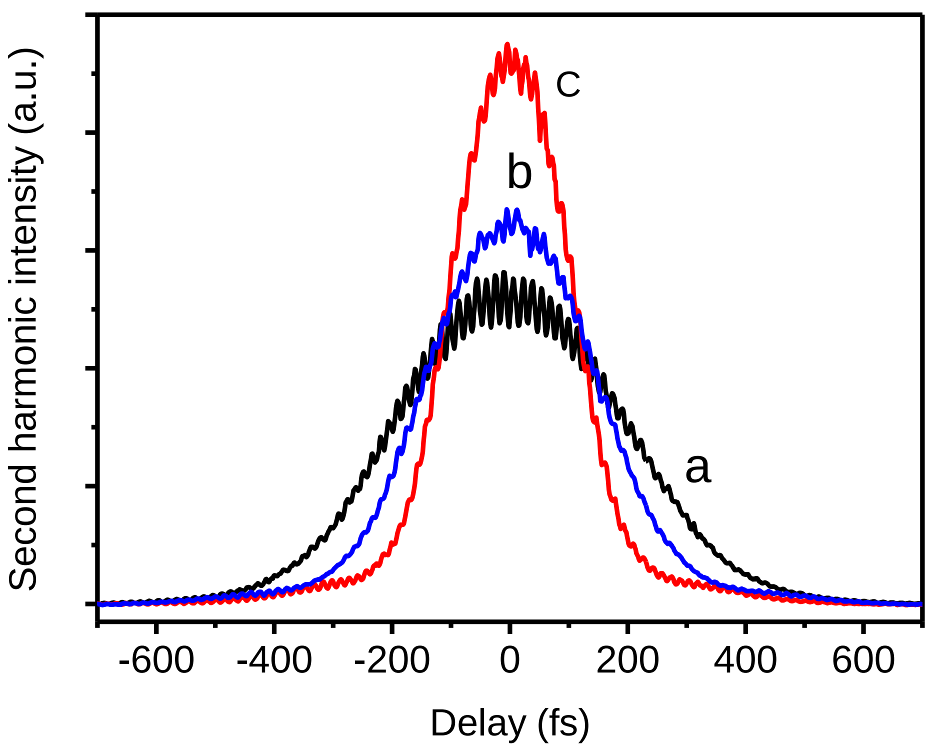

Second harmonic intensity (a.u.)
Delay (fs)
c
b
a
-600
-400
-200
0
200
400
600

Fig.4